Bioresource Technology 441 (2026) 133540

Contents lists available at ScienceDirect

Bioresource Technology

journal homepage: www.elsevier.com/locate/biortech

Acetate co-feeding increases ethylene glycol assimilation and glycolic acid production in *Yarrowia lipolytica*

Eugenia Messina [a], Zbigniew Lazar [b], Serena Barile [a], Paweł Moroz [b], Pasquale Scarcia [a], Ylenia Antonacci [c], Bruno Fosso [a], Luigi Palmieri [a], Isabella Pisano [a], Gennaro Agrimi [a,*]

[a] Department of Biosciences, Biotechnologies and Environment, University of Bari Aldo Moro, Campus Universitario, via Orabona 4, Bari 70125, Italy
[b] Department of Biotechnology and Food Microbiology, Faculty of Biotechnology and Food Science, Wrocław University of Environmental and Life Sciences, Chełmonskiego 37, Wrocław 51-630, Poland
[c] Institute of Biomembranes, Bioenergetics and Molecular Biotechnology, National Research Council, Via Amendola 165/A, Bari 70126, Italy

HIGHLIGHTS

- *Y. lipolytica* cannot grow on EG as the sole carbon source in minimal medium.
- Co-feeding with acetate increases EG uptake and glycolic acid production.
- EG oxidation supplies NADPH, enhances acetate use, and stabilizes pH.
- ^{13}C-MFA shows EG carbon enters biomass via glyoxylate cycle and glycine synthesis.
- Optimized fed-batch strategy yields 48.4 g/L GA with 73 % molar yield.

GRAPHICAL ABSTRACT

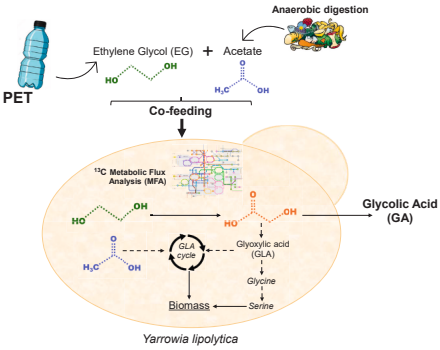

ARTICLE INFO

Keyword:
Plastic upcycling
Ethylene glycol (EG)
Acetate (Ac)
Glycolic acid (GA)
Yarrowia lipolytica
Co-feeding strategies

ABSTRACT

Upcycling ethylene glycol (EG) and terephthalic acid (TPA), key monomers derived from the depolymerisation of polyethylene terephthalate (PET), is a promising strategy for advancing the circular economy of plastics. This study investigates the metabolic fate of EG and its conversion into glycolic acid (GA) by the non-conventional yeast *Yarrowia lipolytica*. While EG alone does not support growth in a minimal medium, the addition of acetate (Ac) significantly enhances EG assimilation and GA production. ^{13}C labeling experiments and metabolic flux analysis revealed that a small but measurable fraction of EG-derived carbon is incorporated into biomass via glycine and serine biosynthesis and the glyoxylate cycle when acetate is supplied as a carbon source. Ac-EG co-feeding resulted in the production of 48.4 ± 1.4 g/L of GA after 66 h, corresponding to a molar yield of 73 % and a productivity of 0.73 g/(L·h). These results highlight the potential of *Y. lipolytica* as a microbial platform for EG valorisation and contribute to sustainable strategies for the bioconversion of plastic waste.

* Corresponding author at: Department of Biosciences, Biotechnologies and Environment, University of Bari Aldo Moro, Campus Universitario, via Orabona 4, Bari 70125, Italy.
E-mail addresses: eugenia.messina@uniba.it (E. Messina), zbigniew.lazar@upwr.edu.pl (Z. Lazar), serena.barile@uniba.it (S. Barile), pawel.moroz@upwr.edu.pl (P. Moroz), pasquale.scarcia@uniba.it (P. Scarcia), y.antonacci@ibiom.cnr.it (Y. Antonacci), bruno.fosso@uniba.it (B. Fosso), luigi.palmieri@uniba.it (L. Palmieri), isabella.pisano@uniba.it (I. Pisano), gennaro.agrimi@uniba.it (G. Agrimi).

https://doi.org/10.1016/j.biortech.2025.133540
Received 14 June 2025; Received in revised form 12 October 2025; Accepted 19 October 2025
Available online 24 October 2025

1. Introduction

Plastic polymers are known for their unique properties such as being lightweight, strong, water-resistant, insulating, and durable (Ilyas et al., 2018). These attributes make them indispensable in almost every aspect of modern life. The first plastic was created in the 1860s, with major industrial advancements occurring in the 1920s. Since then, plastic consumption has surged, with global production hitting 400.3 million tons in 2022 (Nayanathara Thathsarani Pilapitiya and Ratnayake, 2024). However, the short lifespan of plastics often results in poorly managed waste that lingers in the environment due to their non-biodegradable nature, leading to their accumulation in various ecosystems (Kwon et al., 2023). Among all plastics, polyethylene terephthalate (PET) is one of the most widely produced polyesters, commonly used in packaging, textiles, construction materials, automotive parts, and electronic components. Its current global production is around 61 million tons (Ceven and Karakan Gunaydin, 2023; Muringayil Joseph et al., 2024). To address the issue of plastic waste and mitigate the plastic pollution crisis, PET recycling is crucial. Recycling methods include mechanical, chemical, and biorecycling (Muringayil Joseph et al., 2024). Biorecycling employs enzymes to break down PET products into their monomers, terephthalic acid (TPA) and ethylene glycol (EG) (García, 2022). These PET-derived monomers can be used as microbial bioconversion substrates and converted into higher-value products. This approach, known as upcycling, is gaining prominence as an effective strategy for reducing waste and conserving resources (Lomwongsopon and Varrone, 2022; Zhao et al., 2022). One example of this approach is the upcycling of EG to glycolic acid (GA).

Glycolic acid is the smallest two-carbon α-hydroxy acid, featuring both alcohol and acid functional groups. Its versatile chemical profile enables a wide range of applications in the textile (dyeing and tanning agent), food (flavor and preservative), and pharmaceutical industries (skin care agent). GA is also used in industrial and household cleaning products, adhesives, and as an additive in inks and paints to improve flow properties and gloss (Salusjärvi et al., 2019). The global market for GA was valued at USD 302.4 million in 2023 and is projected to grow by 9.6 % from 2024 to 2030 (https://www.grandviewresearch.com/press-release/global-glycolic-acid-market). Currently, GA is chemically synthesized from petrochemical resources, requiring strong acidic or alkaline media and harsh reaction conditions, such as high temperatures and pressures (Si et al., 2021). Moreover, the chemical synthesis of GA is low in selectivity and frequently results in the formation of undesirable by-products due to product decomposition or polymerization (Chauhan et al., 2002, US6416980B1). An alternative is the biological synthesis of GA, which can be efficiently obtained from EG oxidation catalyzed by *Acetobacter* and *Gluconobacter* genera, also known as acetic acid bacteria [AAB], as well as by *Pseudomonas putida* (Kersters and De Ley, 1963; Wei et al. (2009); Mückschel et al., 2012; Zhang et al., 2016; Franden et al., 2018). Previous studies show that AAB microorganisms convert EG to glycolaldehyde and then to GA. In *P. putida*, several redundant NAD(+)- or PQQ-dependent dehydrogenases catalyze the oxidization of EG to GA, which can be further oxidized to glyoxylic acid (GLA) (Mückschel et al., 2012; Li et al., 2019).

Yeast has been reported as a promising biocatalyst of EG to GA biotransformation (Kataoka et al., 2001; Carniel et al., 2023; Senatore et al., 2024; Senatore et al., 2025).

Exploration of yeast biodiversity across ascomycetes and basidiomycetes confirmed that EG-to-GA conversion is a widespread trait; notably, *Scheffersomyces stipitis* displayed superior performance, producing almost 24 g/L of GA in 144 h under nutrient-rich conditions supplemented with glucose and EG (Senatore et al., 2024). The non-conventional yeast *Yarrowia lipolytica* is gaining prominence as an industrial host for biotechnological applications. Its ability to produce GA from EG has been reported (Carniel et al., 2023). Using whole-cell biocatalysis in a rich medium supplemented with EG, the authors achieved a GA titre of approximately 33 g/L. They further proposed that the conversion of EG to GA may involve oxygen-dependent enzymatic reactions, especially those catalyzed by alcohol dehydrogenases and aldehyde dehydrogenases, suggesting that oxygen transfer could represent a critical parameter influencing the efficiency of the bioconversion process (Carniel et al., 2023).

One of the most prominent metabolic traits of *Y. lipolytica* is its ability to utilize a wide range of substrates. Among these, acetate, a volatile fatty acid (VFA), is emerging as an alternative feedstock due to its efficient assimilation and high tolerance by *Y. lipolytica*. Acetate can be sustainably sourced from various processes, including the anaerobic digestion of organic waste (Park et al. (2021)), photocatalytic CO_2 reduction (Zhu et al., 2021), and syngas fermentation (Ciliberti et al., 2020). Currently, acetate is priced at approximately USD 350–450 per ton, making it more cost-effective than conventional carbon sources such as glucose, which is priced around USD 500 per ton (Mutyala and Kim, 2022). Due to its low cost, renewable origin, and non-competition with the food supply chain—unlike carbohydrate- or lipid-based substrates—acetate represents a promising feedstock for industrial microbial fermentation processes aligned with sustainable development goals.

Despite its advantages, acetate utilization currently suffers from limitations, as its catabolism does not directly produce NADPH. To synthesize NADPH, *Y. lipolytica* must convert acetate into glucose via the glyoxylate shunt and gluconeogenesis, as the pentose phosphate pathway (PPP) is the primary source of NADPH in this yeast. This metabolic route is both lengthy and metabolically costly, thereby limiting the efficiency of acetate utilization in *Y. lipolytica* (Liu et al. (2016)). Co-feeding strategies have demonstrated that acetate assimilation can be improved by supplementation with NADPH-generating substrates (Park et al. (2019); Huang et al., 2023). Furthermore, when acetate is used as carbon source, the pH of the culture medium quickly increases to 10, hindering growth rate and resulting in low cell density (Liu et al. (2016)).

In this study, we improved the bioconversion of EG to GA in *Y. lipolytica* by implementing a co-feeding strategy using EG and acetate in a minimal medium. ^{13}C-labeling experiments revealed that under these conditions, EG is primarily oxidized to GA, but a significant fraction is also assimilated into cellular biomass (Fig. 1).

2. Materials and methods

2.1. Strains and culture media

Escherichia coli DH5α and *EcoRed* (Yuzbashev et al., 2023) used for plasmid construction, propagation and amplification, was cultivated in Luria Bertani (LB) media with shaking (200 rpm) at 37 °C and 30 °C, respectively. This medium was supplemented with antibiotics (Sigma-Aldrich, St. Louis, MO, USA) based on the resistance of the plasmids: streptomycin 50 μg/mL; ampicillin 100 μg/mL and kanamycin 50 μg/mL, to allow selective growth. *Y. lipolytica* strains were cultivated in different media at 28 °C and with orbital shaking at 200 rpm. The rich medium, used for seed culture, was YPD medium composed of 1 % (w/v) yeast extract (Biokar Diagnostics, Allonne, France), 2 % (w/v) peptone (Biokar Diagnostics, Allonne, France), and 2 % (w/v) glucose (Sigma-Aldrich, St. Louis, MO, USA). Whenever required, the medium was supplemented with nourseothricin (Jena Bioscience, Jena, Germany) 350 μg/mL for the overnight growth of *Y. lipolytica* strains transformed with Cas9 expressing plasmids. The minimal medium was composed of 0.17 % (w/v) Yeast Nitrogen Base without nitrogen source (YNB) (Difco™, Becton Dickinson, Sparks, MD, USA), 0.5 % (w/v) NH_4Cl and 50 mM phosphate buffer, pH 6.8. Carbon sources employed—glucose, acetate, and/or EG—were administered in varying ratios and concentrations depending on the specific objectives of each experimental setup. For the selection of URA3 marker-based transformants, the minimal medium was supplemented with 2 % (w/v) glucose and 2 g/L of each of the 20 proteinogenic amino acids (Sigma- Aldrich, St. Louis, MO, USA), excluding uracil. Solid media were prepared by adding 1.5 % (w/v) agar

(Type E, Biokar Diagnostics, Allonne, France) to the liquid media. All cultures were maintained at −80 °C in glycerol stocks.

2.2. Construction of plasmids and recombinant strains

Plasmids for yeast genome engineering were constructed using vectors from the synthetic biology toolkit *YaliCraft* (Yuzbashev et al., 2023). Transformation of *Y. lipolytica* strains was performed using the CRISPR/Cas9-based genome editing technique. Specifically, a Cas9-helper plasmid—encoding both Cas9 and a guide RNA (gRNA)—and a repair fragment containing homologous flanking regions for genome integration (Donor) were used.

To inactivate the glyoxylate:alanine aminotransferase gene (*YlAGX1*, YALI1_E19852g), a gRNA targeting *YlAGX1* was designed using the ChopChop tool (https://chopchop.cbu.uib.no/) and inserted in the pCasNA-RK helper plasmid expressing Cas9, as previously described (Yuzbashev et al., 2023), obtaining the plasmid p-M4B582 (Supplementary Materials). Subsequently, the deletion cassette (P-ura3-T *YlAGX1*) was created starting from the PCR amplification of the 595 bp upstream (P cassette) and 505 bp downstream (T cassette) regions of the coding DNA sequence (CDS) from the wild-type strain Y-4972 (W29Δ*ku70*) (Yuzbashev et al., 2023), using specific primers (Supplementary Materials). The P and T cassettes were combined with two Level 0 plasmids of *YaliCraft* toolkit: pYalC-URA3 carrying the URA3 selection marker to restore uracil prototrophy, and pYalK-Bb providing the propagation backbone. Each element is designed with defined overhangs and corresponding *BsaI* restriction sites compatible with Golden Gate assembly (Weber et al., 2011), resulting in the construction of plasmid p-M4B593 (Supplementary Materials). The deletion cassette was subsequently amplified from p-M4B593 and purified with QIAquick® PCR and Gel Cleanup Kit (QIAGEN GmbH, Hilden Germany), generating the donor DNA. The strain Y-4973 (W29Δ*ku70*Δ*ura3*) (Yuzbashev et al., 2023) was transformed using the P-ura3-T *YlAGX1* deletion cassette along with the p-M4B582 plasmid, yielding the engineered strain YM4B5101. The deletion was verified by PCR amplification on the genome of transformant strains using primers flanking the *YlAGX1* gene (Supplementary Materials).

2.3. Shake flask cultures

The ability of *Y. lipolytica* to consume EG, acetate and convert EG to GA was investigated in 250 mL shake flasks. Y-4972 seed culture from YPD plates was grown overnight in 10 mL of YPD medium at 28 °C and 200 rpm. Pre-cultures were centrifuged, washed with sterile distilled water, and inoculated into 50 mL of fresh YNB medium (0.17 % yeast nitrogen base, 0.5 % NH_4Cl, and 50 mM phosphate buffer, pH 6.8) at an initial OD_{600} of 0.1. Sodium acetate and EG were tested as sole carbon sources at a concentration of 20 g/L. For co-feeding experiments, the same YNB medium was used, while varying concentrations of carbon sources: glucose was supplied at 20 g/L, acetate at 20, 30, and 60 g/L, and EG at 20, 30, 40, and 60 g/L. Cultures were incubated at 28 °C and 200 rpm for 10 days. Samples were collected at regular time intervals for OD_{600}, pH and HPLC analysis. To determine dry cell weight (DCW), cultures were washed, frozen and lyophilized in a pre-weighted tube. The weight differences corresponded to the mg of cells present in the dried culture volume. All measurements were performed using at least two biological replicates, and average values with standard errors were calculated.

2.4. Growth conditions for EG and GA toxicity assessment

To test EG and GA toxicity, a single colony of Y-4972 was grown overnight in 10 mL of YPD medium at 28 °C and 200 rpm. Pre-culture was then centrifuged, washed with sterile distilled water, and inoculated in 50 mL shake flasks containing 30 mL of fresh YNB medium (0.17 % yeast nitrogen base, 0.5 % NH_4Cl and 2 % w/v glucose). EG and GA were added at final concentrations of 15, 30 and 60 g/L and a positive control with only glucose was also prepared. The initial pH of the medium was adjusted to 6–6.2 using NaOH. The initial optical density at 600 nm (OD_{600}) was 0.1 and cultures were grown at 28 °C and 200 rpm for 72 h. Growth was monitored by measuring the OD_{600} values every 24 h, and supernatants were collected for HPLC analysis. All

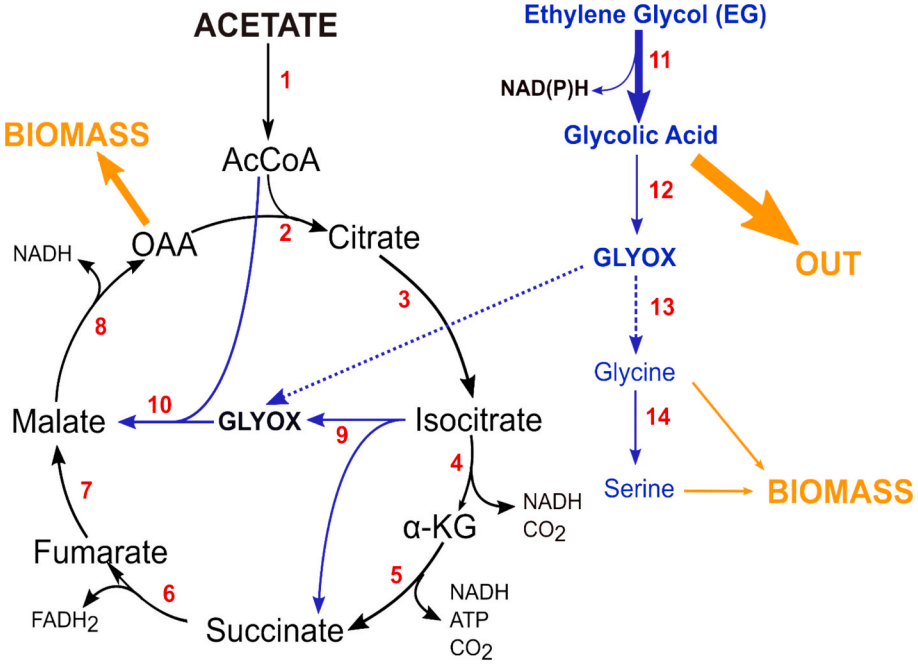

Fig. 1. Diagram of the enzymatic steps involved in the metabolism of acetate (Ac) and Ethylene Glycol (EG). Red numbers indicate the enzymes catalyzing the reactions: 1) Acetate-CoA synthetase; 2) Citrate synthase; 3) Aconitase; 4) Isocitrate dehydrogenase; 5) Alpha-ketoglutarate dehydrogenase and Succinate-CoA ligase; 6) Succinate dehydrogenase; 7) Fumarase; 8) Malate dehydrogenase; 9) Isocitrate lyase; 10) Malate synthase; 11) Alchol and Aldheyde dehydrogenase; 12) Hydroxy acid oxidase; 13) Alanine-glyoxylate amino transferase; 14) Serine hydroxymethyl transferase.

experiments were carried in duplicate and average as well as standard deviations were calculated.

2.5. ^{13}C-labeling experiments

^{13}C-labeling experiments were conducted using *Y. lipolytica* wild-type strain Y-4972 and the deleted strain YM4B5101. Both strains were initially grown in 10 mL pre-culture of YPD medium inoculated from the corresponding plate and incubated overnight at 28 °C and 200 rpm. Pre-cultures were then centrifuged, washed with sterile distilled water, and inoculated in 10 mL of fresh YNB medium (0.17 % yeast nitrogen base, 0.5 % NH_4Cl and 50 mM phosphate buffer, pH 6.8) with an initial OD_{600} of 0.05. EG and sodium acetate (Ac) were supplemented at a final concentration of 20 g/L across three parallel experimental setups: a) presence of 1,2-$^{13}C_2$-EG; b) 1,2-$^{13}C_2$-sodium acetate; c) 1-^{13}C-sodium acetate. For the YM4B5101 strain (*YlAGX1* deletion mutant), only labeling with 1,2-$^{13}C_2$-sodium acetate was performed. All labeled substrates were purchased from Cambridge Isotope Laboratories (MA, USA) with a purity of 99 %. Cultures were incubated at 28 °C and 200 rpm for 168 h. Samples were collected at regular time intervals to monitor OD_{600}, pH, and metabolite profiles using HPLC. Each data point was derived from at least two biological replicates, and average values with standard errors were calculated to ensure statistical reliability.

2.6. Stable isotope analysis using gas chromatography–mass spectrometry (GC–MS)

A culture volume corresponding to an OD_{600} of 1 was centrifuged at 13.000 rpm for 5 min, and the resulting supernatant and cell pellet were stored at −20 °C for subsequent GC–MS analysis. The supernatant was analyzed to assess the contribution of acetate and EG to the production of GA, an extracellular metabolite. The cell pellet was analyzed to evaluate the incorporation of carbon labeled from acetate and EG into amino acids. An aliquot of 5 µL of supernatant was dried using a Techne Dri-Block DB-3A at 80 °C, then resuspended in 30 µL acetonitrile (Optima LC/MS grade, Fisher Chemical), and 30µL *N*-methyl-*N*-*tert*-butyldimethylsilyl-*N*-methyltrifluoroacetamide (MBDSTFA) containing 1 % *tert*-Butyl Dimethyl Chlorosilane (Sigma Aldrich). The reaction proceeded for 1 h at 85 °C, then the sample was analyzed using an Agilent 8890 GC System coupled to an Agilent 5977C MSD. A 1 µL sample volume was injected in splitless mode with the inlet temperature set to 270 °C. Chromatographic separation was achieved using an Agilent J&W HP-5MS-UI column with hydrogen as the carrier gas at a flow rate of 1 mL/min. The GC oven temperature was initially held at 70 °C for 2 min, increased to 90 °C at 3 °C/min, then raised to 300 °C at 15 °C/min, and finally maintained for 3 min. The mass spectrometer operated in electron ionization (EI) mode with an electron energy of 70 eV. The ion source and quadrupole temperatures were set at 230 °C and 150 °C, respectively. Mass spectra were acquired in Full scan mode.

The cell pellet was washed with 500 µL of water, centrifuged at 13.000 rpm for 5 min, and resuspended in 150 µL of 6 M HCl. The suspension was transferred to a glass vial and incubated at 105 °C for 6 h to hydrolyze biomass constituents (Schmitz et al., 2015). After incubation, HCl was evaporated using a heating block at 85 °C under a fume hood. The dried hydrolysate was resuspended in 30 µL acetonitrile and 30 µL MBDSTFA with 1 % *tert*-Butyl Dimethyl Chlorosilane for derivatization. GC-MS analysis was performed as described for GA, with the following modifications: the GC oven temperature was initially set to 140 °C for 1 min, then ramped to 300 °C at a rate of 12 °C/min, and held for 3 min. For precise determination of ^{13}C mass isotopomer distributions of amino acids, spectra were acquired in Selective Ion Monitoring (SIM) mode, as previously reported (Schmitz et al., 2015).

Raw MS data file (.cdf) were processed using PIRAMID, a MATLAB-based tool which integrated target compounds based on retention times, characteristic ions, and isotopologues, providing Mass Isotopomer Distributions (MIDs) corrected for natural isotope abundance (Gomez et al., 2023).

To determine the contribution of 1,2-$^{13}C_2$-labeled EG or acetate to the carbon skeletons of proteinogenic amino acids, a reciprocal ^{13}C-labeling approach was employed, as described by (Christensen and Nielsen, 2002). For this purpose, the Summed Fractional Labeling (SFL) was calculated:

$$\frac{\Sigma\ i x Mi}{\Sigma\ Mi}$$

where M_i represents the mass isotopomer fraction with i indicating the number of ^{13}C-atoms, corrected for the natural abundance of isotopes. The SFL was then normalized by n, the number of carbon atoms in the analyzed fragment, yielding SFL/n. This value reflects the average labeling per carbon atom and indicates the relative contribution of each carbon source to the synthesis of the fragment. For instance, an SFL/n value of 50 % indicates that the fragment is derived equally from both carbon sources.

2.7. ^{13}C-Metabolic flux analysis

The stoichiometric model used for ^{13}C-constrained metabolic flux analysis was constructed based on the core pathways of central carbon metabolism in *Y. lipolytica*, as previously described (Agrimi et al., 2014; Worland et al., 2024). The model comprises 78 fluxes and 57 metabolites, covering the tricarboxylic acid (TCA) cycle, glyoxylate shunt, gluconeogenesis, the PPP, one-carbon metabolism, and amino acid biosynthesis pathways. Gluconeogenic reactions catalyzed by phosphoenolpyruvate carboxykinase and fructose-1,6-bisphosphatase were included, while the pyruvate carboxylase reaction was excluded to prevent futile cycling, in accordance with previous studies (Liu et al. (2016)). Similarly, the pyruvate kinase reaction was omitted from the model. Two pools, cytosolic and mitochondrial, were considered for key intermediates such as citrate, succinate, malate, pyruvate, acetyl-CoA, and oxaloacetate. Additionally, glyoxylate derived from EG and acetate was represented as two distinct pools, connected via an exchange reaction.

Biomass composition was adapted from Pan and Hua (2012), amino acid content and other biomass components from Worland et al., (2024). The complete metabolic network, including carbon atom transitions, is provided in Supplementary Materials.

Flux calculations were performed using the INCA software (Young, 2014), assuming a pseudo-steady state during the 19–72 h growth window. The analysis incorporated MIDs of proteinogenic amino acids and extracellular fluxes, including specific uptake rates of EG and acetate, as well as GA and biomass specific production rates (Supplementary Materials). An uncertainty of 0.2 mol % was assumed for intracellular labeling data. 95 % confidence intervals (CIs) were estimated using INCA's parameter continuation function.

2.8. RNA extraction and transcriptomic analysis

Y. lipolytica Y-4972 strain was cultivated in 50 mL of YNB medium (0.17 % yeast nitrogen base, 0.5 % NH_4Cl, and 50 mM phosphate buffer, pH 6.8) with an initial OD_{600} of 0.1. Two experimental conditions were tested: a) 20 g/L acetate as the sole carbon source; b) co-feeding with 20 g/L acetate and 20 g/L EG. After 65 h of cultivation, total RNA was extracted following the previously described protocol (Messina et al., 2023). The amount of RNA was determined by measuring the absorbance at 260 nm using a NanoDrop 1000 (Thermo Fisher Scientific, Waltham, MA, USA), and purity was assessed by the 260/280 absorbance ratio with acceptable values ranging from 1.8 to 2.0. An additional *DNase* treatment was included to ensure complete removal of DNA.

RNA-seq libraries were prepared from 300 ng of RNA, using the Illumina Stranded mRNA Kit (Illumina, San Diego, CA, USA), according to the manufacturer protocol. cDNA libraries were checked on the

Agilent Bioanalyzer with DNA kit 1000. Sequencing was performed on the Illumina NovaSeq 6000 platform by using a Paired-Ends (PE) layout with 200 cycles.

RNA-seq data analysis was conducted as described in detail in Supplementary Materials. Briefly, raw sequencing reads were trimmed to remove low-quality bases, adapters, and noise, then aligned to *Y. lipolytica* strain CLIB89 W29 reference genome. Gene-level expression quantification was performed using the featureCounts tool from the Subreads package (v2.1.1) (Liao et al., 2019). Statistical analyses were carried out in the R environment (v4.3.3), and multiple testing correction of P-values was applied using the Benjamini-Hochberg (BH) method. Fungal Gene Set Enrichment Analysis (GSEA) was performed using the FunFea R package (Charest et al., 2025).

2.9. Metabolites quantification by HPLC

HPLC analysis was performed to quantify the amount of glucose, EG, GA, and acetate. Prior to analysis, culture supernatants were centrifuged at 12.000 rpm for 10 min and diluted when necessary. The HPLC system used was a Nexera Lita (Shimadzu), equipped with a Resex ROA-Organic Acid H+ (8 %) column (300 mm x 7.8 mm, Phenomenex). A sample volume of 10 µL was injected into the column. The mobile phase consisted of 0.01 M H_2SO_4, delivered at a flow of 0.6 mL/min, with the column maintained at 65 °C. Separated components were detected by a variable wavelength detector set at 210 nm (Photodiode Array Mod. Shimadzu SPD-M40), and a refractive index detector (Shimadzu RID-20A). Peaks were identified by comparison with reference standards dissolved in ultrapure water. Calibration curves for peak quantification were constructed over a concentration range of 0.1–12 g/L.

2.10. Production of GA by Y. lipolytica in bioreactor

Y. lipolytica Y-4972 strain was grown in 5 L bioreactor (BIOSTAT B Plus; Sartorius, Germany) with an initial working volume of 1 L. The temperature was kept constant at 28 °C and pH was set to 6.5, maintained by automatic addition of 30 % KOH and 10 M HCl. The agitation rate was 800 rpm and filtered air was continuously sparged through the reactor at a flow rate of 0.8 vvm. Seed cultures from YPD plates were grown for 24 h in 10 mL YPD at 28 °C and 200 rpm. For the inoculum, cells were harvested, washed with sterile distilled water and used to inoculate the bioreactor with a starting OD_{600} of 1. GA was produced in YNB 1.7 g/L and NH_4Cl 5 g/L dissolved in tap water. Two co-feeding strategies were evaluated. In the first, fermentation was initiated with 50 g/L acetate and 10 g/L EG, followed by pulsed additions of 10 g/L EG at 24 and 48 h. In the second strategy, 50 g/L EG and 10 g/L acetate were supplied at the start, with subsequent pulses of 10 g/L acetate at the same time points. In both strategies, a total of 30 g/L of either acetate or EG was pulsed, resulting in a combined concentration of 80 g/L of both substrates in each co-feeding experiment.. Samples were collected at regular time intervals for OD_{600}, DCW measurement, and HPLC analysis. Two independent replicates were performed. Yield (Yp/s) was determined by molar ratio of GA formed (product) and EG consumed (substrate).

2.11. Data analysis

All experiments were performed in at least two biological replicates, and results are presented as average ± standard error to ensure statistical reliability. Graphical data visualizations and statistical analyses were performed using GraphPad Prism v.10. Differences between experimental groups were assessed using the unpaired Student's *t*-test, with significance defined as P-value < 0.05 (*P < 0.05; **P < 0.01; ***P < 0.001).

3. Results

3.1. Acetate stimulates EG utilization in Y. lipolytica

Y. lipolytica cannot utilize EG as its sole carbon source, as evidenced by the lack of growth on minimal medium containing only EG (20 g/L). Despite inoculum concentrations of 0.5 OD_{600}, no growth was observed after 140 h of cultivation. However, HPLC analysis showed a gradual reduction of EG, with volumetric consumption rates of 0.01 ± 0.00 g/(L·h) and 0.05 ± 0.01 g/(L·h) for inocula of 0.1 and 0.5, respectively. Concurrently, a peak corresponding to GA appeared, with concentrations of 2.3 ± 0.2 g/L and 3.1 ± 0.2 g/L for inocula of 0.1 and 0.5, respectively, after 140 h (Supplementary Materials). These results suggest that EG bioconversion to GA is catalyzed and occurs independently of cell growth, as previously reported (Carniel et al., 2023). Franden et al., (2018) demonstrated that the soil bacterium *Pseudomonas putida* KT2440 can oxidize EG to GA, which is subsequently converted to GLA. As with other C2 compounds, GLA cannot support biomass formation unless it is further metabolized into C4 intermediates, such as malate, via condensation with acetyl-CoA in a reaction catalyzed by malate synthase (Fig. 1). It is highly plausible that *Y. lipolytica*, like other yeasts, follows a similar metabolic pathway, oxidizing EG to GA and then to GLA. This metabolic route likely explains its inability to grow in minimal medium with EG as the sole carbon source, due to a bottleneck in the conversion of C2 compounds into C4 intermediates required for biomass synthesis.

To overcome this limitation and enhance EG metabolism, we supplemented the medium with both EG and acetate. The latter supports the glyoxylate cycle, enabling the production of C4 compounds essential for anabolic processes and biomass formation (Fig. 1).

The growth of *Y. lipolytica* was evaluated in shake flasks containing a minimal medium with 20 g/L of both EG and acetate, using an inoculum concentration of 0.1 OD_{600nm} (Fig. 2A). The presence of acetate markedly enhanced EG consumption, reaching a rate of 0.11 ± 0.03 g/(L·h), approximately 11-fold higher than when EG was supplied as the sole carbon source (Table 1). These results suggest that acetate plays a crucial metabolic role by supporting more efficient EG oxidation.

Acetate was completely consumed in 140 h (Fig. 2A) with a rate of 0.18 ± 0.03 g/(L·h). Following acetate depletion, both cell growth and EG consumption significantly decreased (Fig. 2A), confirming the synergy between the two substrates. *Y. lipolytica* grew up to 5.0 ± 0.2 g/L DCW, leading to a biomass yield of 0.15 g/g (gDCW/gAc) and 0.09 g/g (gDCW/gAc + gEG) (Table 1). The pH of the medium did not change significantly throughout the fermentation, with a final value of 7.0 ± 0.5. After 240 h, *Y. lipolytica* produced 19.7 ± 0.7 g/L of GA through EG oxidation (Fig. 2A), achieving a final molar yield ($Y_{GA/EG}$) of 0.91 mol/mol (Table 1).

In a parallel experiment, the ability of *Y. lipolytica* to utilize 20 g/L acetate as the sole carbon source was evaluated in shake flask cultures using minimal medium. Under these conditions, the strain exhibited a lag phase of approximately 24 h before growth commenced (Fig. 2B). The culture reached a maximum biomass concentration of 2.3 ± 0.5 g/L DCW, representing a significant 54 % reduction compared to the EG + Ac condition ($P < 0.001$) (Table 1). Over 140 h, 16.6 ± 0.4 g/L of acetate was consumed, corresponding to a consumption rate of 0.13 ± 0.01 g/(L·h) and a biomass yield of 0.12 gDCW/gAc (Table 1), which were 1.4- and 1.2-fold lower, respectively, than those observed under EG and acetate co-consumption. Notably, the pH of the medium increased from 8.5 to 12 during fermentation (Fig. 2B), a shift that likely hindered cell growth.

To investigate whether other carbon sources could also stimulate EG utilization, a co-culture experiment was conducted using glucose and EG (20 g/L). Under these conditions, EG consumption rate was 0.06 ± 0.00 g/(L·h), half of the rate observed in the acetate + EG co-culture (Table 1). The percentage of conversion of EG to GA was lower, reaching only 36 % compared to 86 % in the acetate + EG condition. In the

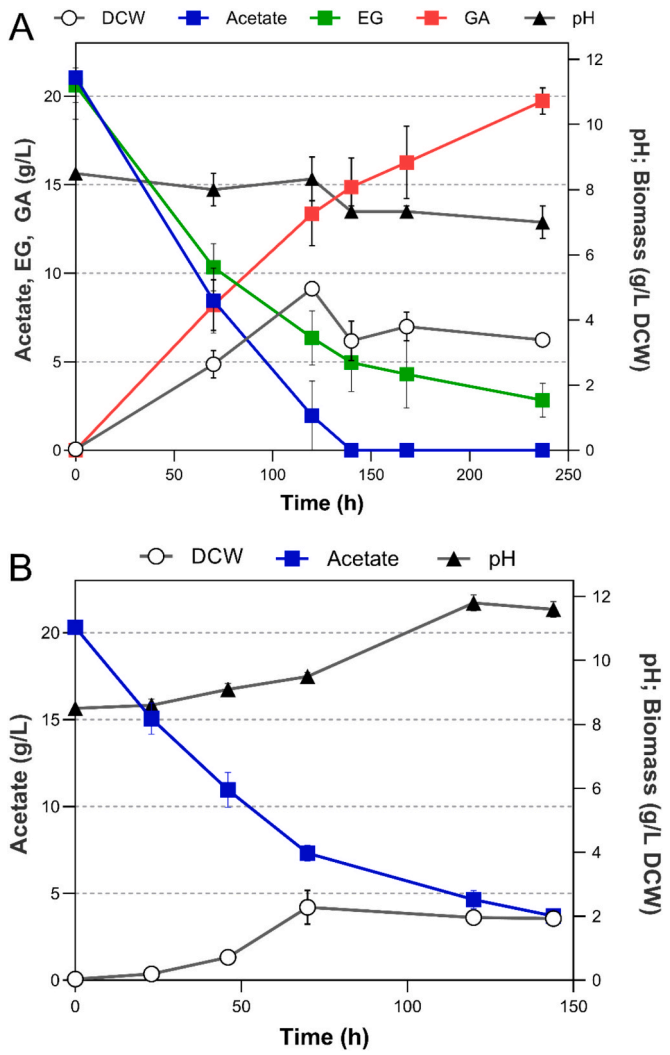

Fig. 2. (A) Growth and EG bioconversion to GA by Y-4972 strain on YNB medium + Ac 20 g/L + EG 20 g/L. Cells were grown for 240 h at 28 °C and 200 rpm. (B) Growth of Y-4972 strain on YNB medium + Ac 20 g/L for 164 h at 28 °C and 200 rpm. g/L of DCW (Dry Cell Weight – white circles), g/L of Ac (blue squares) and EG (green squares) consumed, g/L of GA produced (red squares) and pH (black triangles). Average and standard errors were obtained from at least three replicate experiments.

glucose + EG condition, bioconversion was likely impaired by a pH drop to 2.5 (Table 1), resulting from the production of organic acids – a typical metabolic trait of *Y. lipolytica* when cultivated on glucose. The final titer of GA was 6.1 ± 0.1 g/L (Supplementary Materials), which was 3 times lower than the amount obtained from co-feeding with acetate and EG, and the final molar yield ($Y_{GA/EG}$) was 0.68 mol/mol (Table 1). Acetate was more effective than glucose in stimulating EG utilization and its bioconversion into GA in *Y. lipolytica*.

Across all experiments, EG bioconversion to GA occurred with a molar ratio of GA/EG < 1 (Table 1), meaning that the whole EG consumed, for all cultivations, exceeded the amount of GA produced. These findings led us to speculate that EG not converted into GA could be used by *Y. lipolytica* to produce CO_2, biomass, or other metabolites.

3.2. Tracing the fate of EG through ^{13}C labeling experiments and metabolic flux analysis

To evaluate whether EG not directed toward GA synthesis contributes to biomass formation, ^{13}C-labeling experiments were conducted. Two parallel fermentations were performed, each containing 20 g/L of both substrates. In each experiment, a different ^{13}C-labeled compound was used: 1,2-$^{13}C_2$-acetate in the first, and 1,2-$^{13}C_2$-EG in the second. ^{13}C enrichment in GA and proteinogenic amino acids was analyzed during the late fermentation phase (168 h), when acetate was fully depleted and EG consumption had nearly ceased (Fig. 2A).

As anticipated and illustrated in Fig. 3A, GA was derived almost exclusively from EG. Interestingly, we observed that ^{13}C-EG labeled all the measured proteinogenic amino acids (Supplementary Materials). To quantify the contributions of EG and acetate to amino acid biosynthesis individually, a reciprocal ^{13}C-labeling strategy was employed. Summed fractional labeling per carbon atom (SFL/nC) was calculated according to the method described by (Christensen and Nielsen, 2002). This parameter reflects the average ^{13}C enrichment per carbon atom and serves as a direct indicator of the carbon source used in the synthesis of amino acid backbones. The results revealed near-complete reciprocal labeling, with the combined ^{13}C contributions from EG and acetate approaching unity, thereby validating the robustness of the approach.

Notably, EG-derived labeling was prominent in glycine and serine where almost half of the carbon skeleton was derived from this labeled substrate (Fig. 3B). In *Saccharomyces cerevisiae*, glycine biosynthesis has been reported to occur via transamination of glyoxylate, catalyzed by a Alanine:Glyoxylate aminotransferase (*AGX1*) (Schlösser et al., 2004). Serine biosynthesis likely proceeds via serine hydroxymethyltransferase (*SHMT*), utilizing glycine as a precursor. To elucidate the biochemical mechanisms by which EG-derived glyoxylate is involved in the biosynthesis of glycine and serine, we deleted the gene YALI1_E19852g, which encodes a putative glyoxylate:alanine aminotransferase sharing 45 % amino acid identity with *Saccharomyces cerevisiae* Agx1. The resulting mutant strain, YM4B5101 (Δ*YlAGX1*), showed a significant increase in ^{13}C-acetate-derived labeling of proteinogenic amino acids, most notably glycine and serine, indicating a ~ 50 % reduction in EG-derived carbon incorporation (Fig. 3C). These findings highlight the functional relevance of *YlAGX1* in EG assimilation and its contribution to amino acid

Table 1
Growth and production parameters of *Y. lipolytica* grown on YNB medium (0.17 % yeast nitrogen base, 0.5 % NH_4Cl and 50 mM phosphate buffer, pH 6.8) with only EG or Ac, EG + Ac and Glucose + EG. Cultures were maintained at 28 °C and 200 rpm. Average and standard errors wereobtained from at least two replicate experiments. *** Indicates g/L of DCW of only-Ac culture, significantly different from that of EG + Ac culture. Statistical significance was assessed using an unpaired Student's *t*-test (*** $P < 0.001$).

Condition	EG consumption rate [g/(L·h)] 140 h	Ac consumption rate [g/(L·h)] 140 h	Ac consumed (g/L) 140 h	Max DCW (g/L)	Y(gDCW/gAc) [g/g] 140 h	Y(DCW/gAc + gEG) [g/g] 140 h	Final pH	GA (g/L) 240 h	Y(GA/EG) [mol/mol] 240 h
EG 20 g/L	0.01 ± 0.00		N.D.				6.5 ± 0.0	2.3 ± 0.2	
Ac 20 g/L + EG 20 g/L	0.11 ± 0.03	0.18 ± 0.03	20.0 ± 0.0	5.0 ± 0.2	0.16	0.09	7.0 ± 0.5	19.7 ± 0.7	0.912
Ac 20 g/L		0.13 ± 0.01	16.6 ± 0.4	2.3 ± 0.5***	0.12		11.6 ± 0.2		
Glu 20 g/L + EG 20 g/L	0.06 ± 0.00			7.9 ± 0.2			2.5 ± 0.0	6.1 ± 0.1	0.68

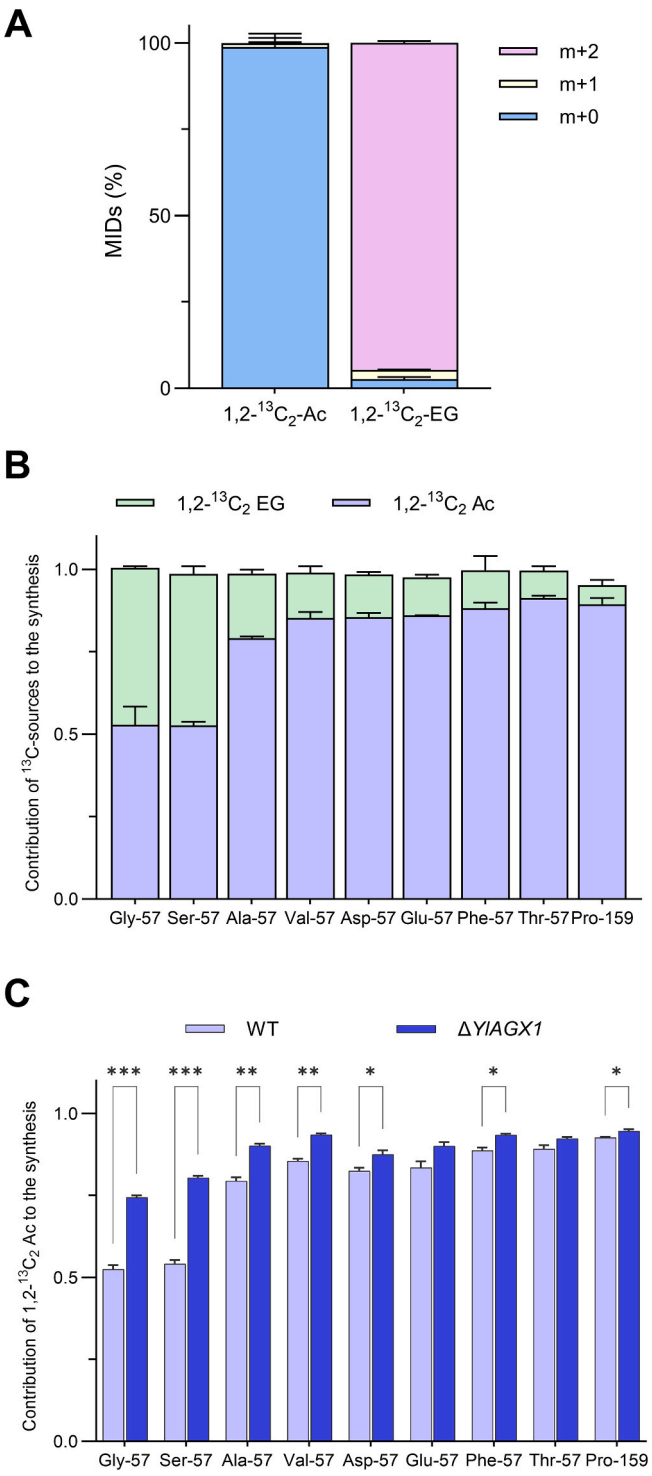

Fig. 3. Carbon labeling analysis after 168 h of cultivation of *Y. lipolytica* in a medium supplemented with ^{13}C-labeled Ac (20 g/L) and EG (20 g/L).“ (A) Distribution of mass isotopomers of GA. (B) Contribution of 1,2-$^{13}C_2$-EG or 1,2-$^{13}C_2$-Ac to the synthesis of the carbon backbone of proteinogenic amino acids. Displayed values represent the Summed Fractional Labeling (SFL) of each amino acid, normalized to the number of carbon atoms in the backbone. SFL was derived from mass isotopomer distributions (MIDs), corrected for natural isotope abundance, as detailed in the Methods section. (C) Quantitative evaluation of the contribution of 1,2-$^{13}C_2$-Ac to the biosynthesis of carbon backbones in proteinogenic amino acids in *Y. lipolytica* wild-type and YM4B5101 (Δ*YlAGX1*) strains.

biosynthesis.

EG also played a significant role in the synthesis of alanine, with approximately 25 % of its carbon skeletons labeled in the presence of ^{13}C-EG (Fig. 3B). Although the carbon labeling in other amino acids containing four or more carbon atoms was below 10 %, it still clearly demonstrated the incorporation of EG into yeast biosynthetic pathways (Fig. 1).

To systematically investigate EG–acetate co-metabolism, a ^{13}C-metabolic flux analysis (^{13}C-MFA) was conducted during the early growth phase (19–72 h), when both carbon sources were actively co-utilized, and biomass accumulation was observable (Fig. 2A). A metabolic network model was constructed, involving key reactions from central carbon metabolism, amino acid biosynthesis, biomass formation, and EG degradation pathways. To improve flux resolution, a third parallel co-feeding labeling experiment was conducted using 1-^{13}C-acetate as the labeled substrate.

Flux distributions were estimated based on substrate uptake rates (EG and acetate) and the mass isotopomer distributions (MIDs) of proteinogenic amino acids. The model was developed under the following key assumptions: a) The reaction involving the conversion of glyoxylate, derived from EG, into glycine, catalyzed by *YlAGX1*, was included into the model; b) Two distinct glyoxylate pools were considered, one from acetate and one from EG, connected via an exchange reaction, with a net flux directing EG-derived glyoxylate into central metabolism; c) A direct serine-to-pyruvate conversion was incorporated, potentially catalyzed by serine dehydratase.

Model predictions showed good agreement with experimental data, with a sum of squared residuals (SSR) of 115, falling within the expected range of 76–132, thereby supporting the validity of the flux estimations.

The obtained flux distribution (Fig. 4) indicates that during this growth phase approximately 7 % of the carbon from EG was assimilated into central metabolism – around 5 % via the glyoxylate cycle and 2 % through glycine and serine biosynthesis. The remaining EG was secreted as GA. The model further suggested that the oxidation of EG to GA may utilize NADPH rather than NADH as a cofactor. As a result, both gluconeogenic flux and NADPH generation via the oxidative PPP were substantially reduced in the simulated flux distribution, compared to those observed in *Y. lipolytica* grown exclusively on acetate. For example, Liu et al. (2016)) reported that approximately 10 % of acetate was directed toward NADPH production via the PPP, whereas in our study this contribution was reduced to approximately 1 %. These findings suggest that comparable NADPH levels are maintained through distinct metabolic pathways when cells are grown in acetate alone versus acetate combined with EG.

Notably, statistically acceptable flux estimations were only achieved when the model incorporated an exchange reaction between the glyoxylate pools derived from acetate and EG. This suggests metabolic connectivity between these pools. Collectively, these findings provide the first direct evidence of a plastic-derived building block being incorporated into yeast biomass and offer a detailed characterization of its metabolic fate.

3.3. Transcriptomic-based analysis of ethylene glycol and acetate co-utilization

The transcriptomic profiles of strain Y-4972 were analyzed under two substrate conditions: (i) 20 g/L acetate (Ac), and (ii) 20 g/L acetate supplemented with 20 g/L ethylene glycol (Ac + EG). The aim was to identify candidate genes potentially involved in EG metabolism. To mitigate the biological variability and assess gene-expression differences between the tested conditions, transcriptome analysis was exploited using four biological replicates per condition, designated as GA1–GA4 for acetate and GA5–GA8 for acetate + EG.

A significant reprogramming of the *Y. lipolytica* transcriptome was observed under acetate + EG co-culture condition. Principal Component Analysis (PCA) revealed a distinct separation of the transcriptomic

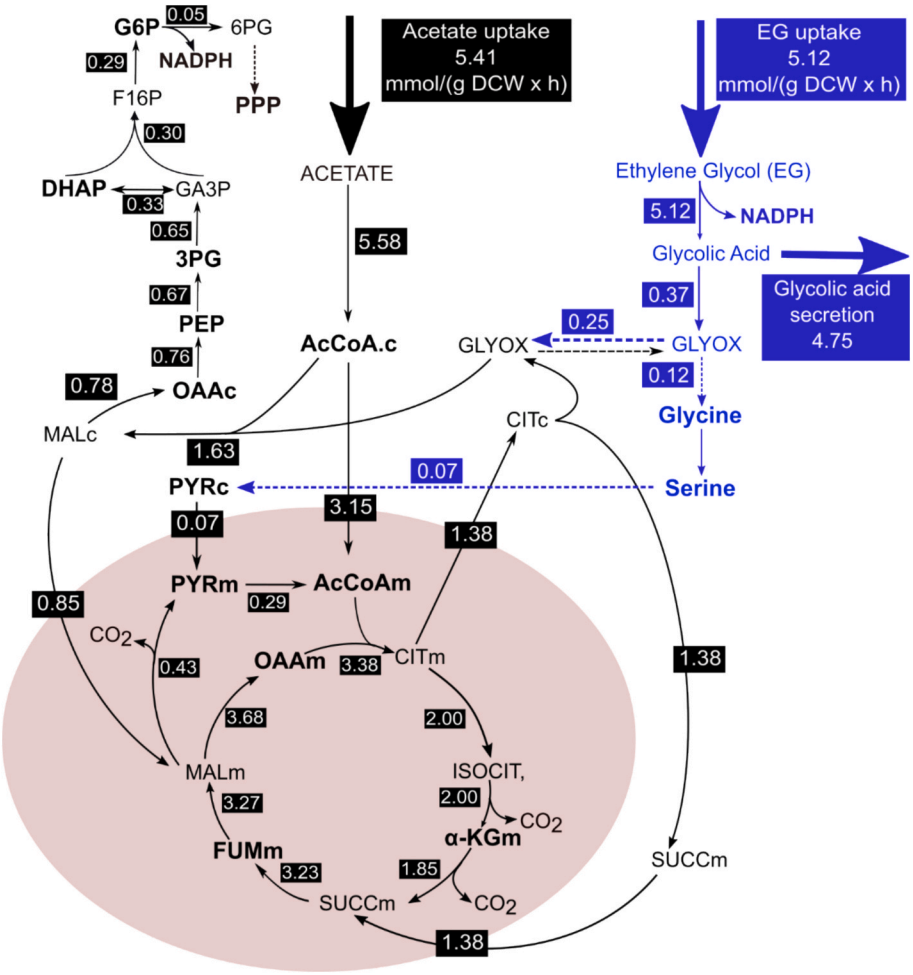

Fig. 4. Flux distributions obtained from ^{13}C-metabolic flux analysis during the co-utilization of Ac and EG. The values shown within the colored boxes represent best-fit flux estimates, expressed in mmol/(g DCW·h). For clarity, only reactions central to Ac and EG metabolism are depicted. Complete flux distributions, along with associated confidence intervals, are available in Supplementary Materials. Metabolites shown in bold directly contribute to biomass synthesis. Dashed arrows indicate hypothetical reactions incorporated to improve model fit with experimental data.

profiles. The first principal component, accounting for 90 % of the total variance, clearly distinguished between the acetate-only and acetate + EG conditions. The second component, explaining 5 % of the variance, captured variability within each group and was primarily influenced by two samples (GA4 and GA7), which had the highest number of fragments used for gene expression quantification (Fig. 5A).

Out of the 8,574 expressed genes, 4,190 were found to be differentially expressed between the two growth conditions. Specifically, 2,082 genes were upregulated in the acetate-only condition, while 2,108 genes showed increased expression under the acetate + EG condition (Fig. 5B).

A Gene Set Enrichment Analysis (GSEA) based on three annotation ontologies, namely KOG (euKaryotic Orthologous Groups) (Tatusov et al., 2003), GO (Gene Ontology) (Ashburner et al., 2000; Gene Ontology Consortium et al., 2023), and KEGG (Kanehisa and Goto 2000), was performed. All the performed enrichment analysis (Supplementary Materials) revealed a significant overrepresentation of metabolism-related terms in *Y. lipolytica* cells cultivated on acetate + EG.

Gene Ontology (GO) enrichment analysis for *Y. lipolytica* grown on acetate + EG highlighted a pronounced overrepresentation of oxidoreductase activities, specifically those acting on aldehyde or oxo groups with NAD^+ or $NADP^+$ as electron acceptors. Notably enriched functions included formate dehydrogenase (NAD^+) and alcohol dehydrogenase [$NAD(P)^+$] activity. Additional enriched categories involved manganese ion transmembrane transporter activity and ferric-chelate reductase activity. Importantly, glutathione-disulfide reductase (NADPH) activity and general antioxidant functions were significantly upregulated under the acetate + EG condition (Fig. 5C). These findings suggest that co-exposure to acetate and EG predominantly induces genes associated with oxidative metabolism and cellular redox balance.

The observed upregulation of multiple alcohol and aldehyde dehydrogenases (Table 2) indicates that EG metabolism likely involves a diverse set of enzymatic activities, rather than being driven by a single dominant enzyme. Among these, alcohol dehydrogenases (YALI1D33961g – *YlADH1*, YALI1D09034g and YALI1F12666g), D-lactate dehydrogenase (YALI1E03870g – *YlDLD1*), and aldehyde dehydrogenases (YALI1E00588g and YALI1F06858g) (Table 2) stand out due to their significantly elevated expression in the presence of acetate and EG, along with high normalized expression levels. These enzymes are promising candidates for metabolic engineering strategies aimed at enhancing EG oxidation. Interestingly, several formate dehydrogenase genes, including YALI1F18740g and YALI1A12540g (Table 2), were also notably overexpressed in the Ac + EG condition, despite no prior literature directly linking them to EG or its intermediates. This unexpected expression may point to secondary oxidative pathways, such as the conversion of glyoxylate to CO_2 and formate, potentially triggering the activation of these genes (Chen et al., 2024). Additionally, the presence of EG appears to induce the overexpression of genes associated with antioxidant responses, such as YALI1E21406g encoding a putative glutathione reductase and YALI1C23738g encoding a putative

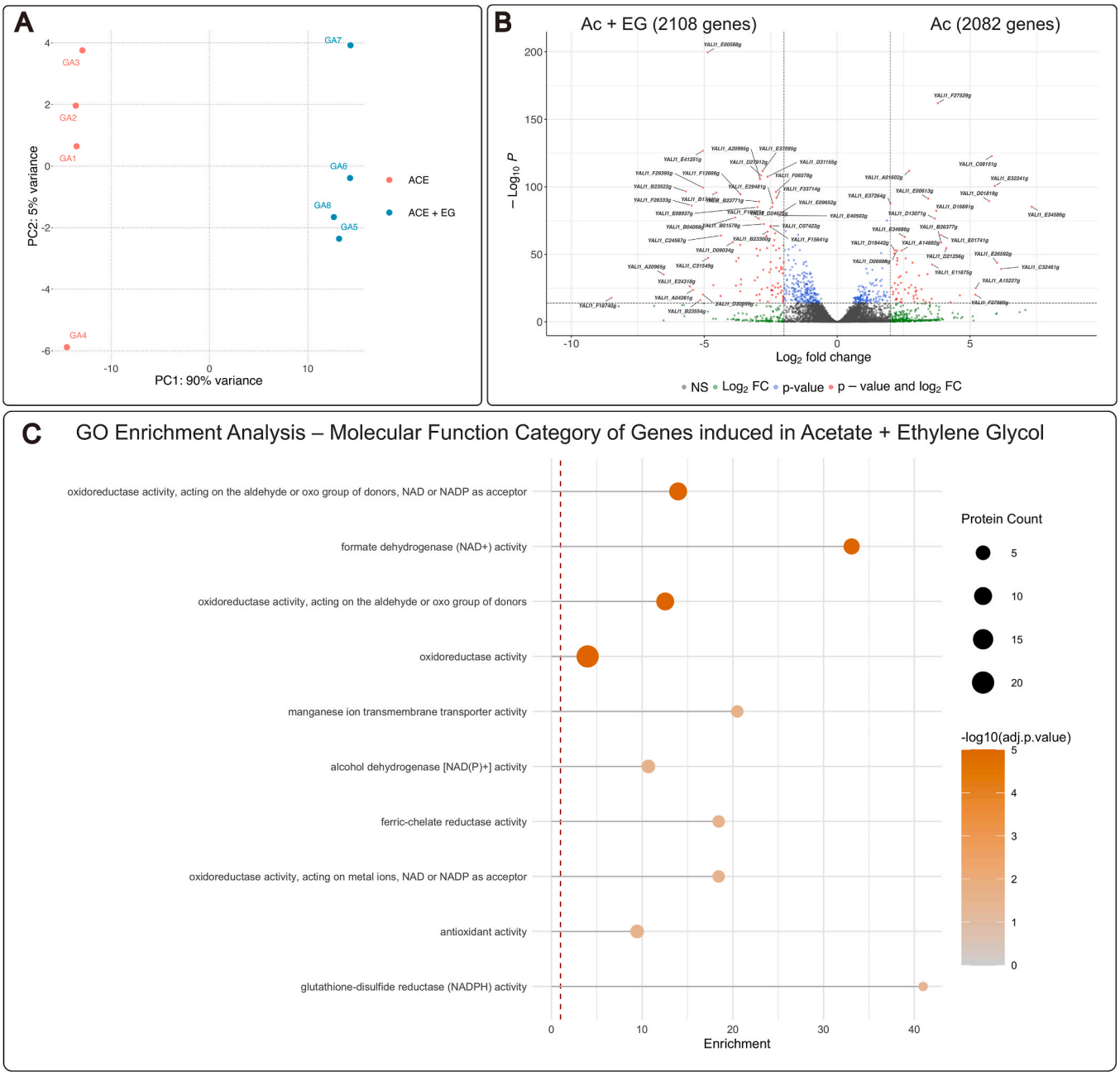

Fig. 5. (A) Principal Component Analysis (PCA) performed on normalized gene expression counts, illustrating sample clustering under two growth conditions: acetate plus ethylene glycol (Ac + EG) and acetate alone (Ac). (B) Volcano plot of differentially expressed genes (DEGs) comparing Ac versus Ac + EG. The plot displays $\log_2$ fold change (FC) against $-\log_{10}$ adjusted P-value. Genes with $\log_2$ FC ≥ 2 are considered upregulated in the Ac condition, while those with $\log_2$ FC ≤ -2 are upregulated in the Ac + EG condition. For clarity, only genes with adjusted P-values $\leq 1 \times 10^{-12}$ are shown. (C) Gene Ontology (GO) enrichment analysis highlighting molecular functions significantly enriched among genes upregulated in the Ac + EG condition.

manganese superoxide dismutase (Table 2), suggesting that EG oxidation generates excess reducing power, thereby eliciting an enhanced oxidative stress response.

3.4. Production of GA with Y. lipolytica in bioreactors

In the presence of acetate, *Y. lipolytica* efficiently converts EG into GA, while its conversion into biomass is less efficient. Considering that GA is a highly valuable molecule with a market price significantly higher than EG, we shifted our focus towards optimizing conditions to enhance GA production.

Preliminary experiments were carried out to assess the toxicity of both the substrates and the resulting product of this biotransformation. To evaluate the toxicity of EG, *Y. lipolytica* was cultured with 20 g/L of glucose and varying concentrations of EG. Cell growth was not impacted by EG concentrations up to 60 g/L, as evidenced by the DCW at 72 h, which reached 5.1 ± 1.1 g/L, closely matching the control condition without EG (5.5 ± 3.0 g/L). (Supplementary Materials). The initial pH, ranging between 6 and 6.2, declined to approximately 1 across all culture conditions. Similarly, *Y. lipolytica* exhibited no adverse effects when exposed to GA concentrations up to 30 g/L, achieving a final DCW of 6.6 ± 3.4 g/L after 72 h, comparable to the positive control without GA. However, at 60 g/L of GA, growth slowed, yielding a final DCW of 3.6 ± 0.7 g/L. This suggests that, while *Y. lipolytica* can tolerate GA levels of 60 g/L, its growth is reduced. Notably, whereas the pH of cultures containing only glucose declined to 1 within 24 h, the pH of cultures

Table 2
Estimated fold change values and functional annotations of selected transcripts. The column 'Log2(FC)' reports the $\log_2$ fold change for the comparison between acetate (Ac) and acetate plus EG (Ac + EG) growth conditions, while the corresponding adjusted p-values are listed under 'Padj'. Normalized counts, reflecting the number of reads mapped to each gene, are shown in the 'Norm. counts' column. Only genes with higher expression under Ac + EG conditions are included. Functional annotations were obtained from GRYC (Genome Resources for Yeast Chromosomes – https://gryc.inrae.fr/) and UniProt (https://www.uniprot.org/).".

Transcript	Functional annotation	Log_2(FC)	P_{adj}	Norm. counts
YALI1_D33961g (*YlADH1*)	uniprot|Q9UW08 *Yarrowia lipolytica* Alcohol dehydrogenase 1	−4.56	5.00E-13	1414.53
YALI1_D09034g	similar to uniprot|P53111 *Saccharomyces cerevisiae* YGL157w, NADPH-dependent aldehyde reductase ARI1	−3.94	1.25E-59	20750.48
YALI1_F12666g	similar to uniprot|P53111 *Saccharomyces cerevisiae* YGL157w, NADPH-dependent aldehyde reductase ARI1 and DEHA0A06347g *Debaryomyces hansenii*	−3.64	3.58E-95	1215.90
YALI1_A21000g	similar to uniprot|P47137 *Saccharomyces cerevisiae* probable oxidoreductase YJR096W	−3.00	1.02E-33	1453.46
YALI1_E03870g (*YlDLD1*)	similar to uniprot|P32891 *Saccharomyces cerevisiae* YDL174c DLD1 D-lactate dehydrogenase (cytochrome) 1, mitochondrial	−2.63	5.21E-26	1962.21
YALI1_E00588g	similar to uniprot|P46367 *Saccharomyces cerevisiae* YOR374w ALD4 potassium-activated aldehyde dehydrogenase, mitochondrial	−4.87	2.22E-200	9858.70
YALI1_F06858g	similar to uniprot|P40047 *Saccharomyces cerevisiae* YER073w ALD5 aldehyde dehydrogenase (NAD +) mitochondrial; similar to *S. cerevisiae* ALD6 (YPL061W)	−1.30	1.05E-12	7366.97
YALI1_F18740g	highly similar to uniprot|O93968 *Candida boidinii* Formate dehydrogenase or uniprot|O13437 *Candida boidinii* NAD-dependent Formate dehydrogenase	−8.49	1.59E-18	3748.16
YALI1_A12540g	highly similar to uniprot|O93968 *Candida boidinii* Formate dehydrogenase	−3.04	5.71E-13	47364.42
YALI1_E21406g	similar to uniprot|P41921 *Saccharomyces cerevisiae* YPL091w GLR1 glutathione reductase (NADPH)	−2.50	1.19E-39	50485.27
YALI1_C23738g	similar to uniprot|P00447 *Saccharomyces cerevisiae* YHR008c SOD2 superoxide dismutase (Mn), mitochondrial	−3.55	6.13E-07	3989.26
YALI1_A15132g	similar to uniprot|P25297 *Saccharomyces cerevisiae* YML123c	−3.65	1.23E-57	1021.21
YALI1_B17441g	PHO84 Inorganic phosphate transporter; also exhibits manganese ion transmembrane transporter activity strong similarity to uniprot|P36033 *Saccharomyces cerevisiae* YKL220c FRE2 Ferric/cupric reductase transmembrane component 2	−4.55	1.87E-96	3900.70

with GA remained stable between 5 and 6 (Supplementary Materials).

To optimize GA production in *Y. lipolytica*, we conducted experiments in shake flasks with varying concentrations of acetate and EG. Regardless of the tested conditions, GA production remained unchanged, consistently achieving a titer of about 20 g/L in all cases (Supplementary Materials). Our observations indicated that at an initial acetate concentration of 20 g/L, the biotransformation of EG to GA was primarily limited by the depletion of acetate (Fig. 2A). An increase in the initial acetate concentration resulted in a prolonged lag phase. At the highest tested level (60 g/L), biotransformation was hindered due to the alkalinization of the medium (Supplementary Materials).

Recognizing the significance of pH control and the necessity of a feeding protocol, as demonstrated by shake flask experiments, we opted to investigate GA production using EG and acetate with *Y. lipolytica* in stirred tank reactors. This approach involved two co-feeding strategies where one substrate was initially supplied at higher concentrations, while the second substrate was added in pulses every 24 h.

In the first strategy, acetate was added at the beginning of fermentation at a concentration of 50 g/L. At time zero, EG was present at a concentration of 10 g/L; every 24 h, 10 g/L of EG was added to the medium (Fig. 6A). Since the fermentation lasted 72 h, a total of 30 g/L of EG was pulsed. Acetate was completely depleted after 48 h, resulting in 9.1 ± 0.5 g/L of DCW (Fig. 6A) and a yield ($Y_{DCW/Ac}$) of 0.18 g/g. EG consumption was about 4.5 g/L every 24 h. At the end of cultivation, 14.4 ± 1.7 g/L of EG was consumed, leading to the production of 17.4 ± 2.0 g/L of GA (Fig. 6A). The final molar yield ($Y_{GA/EG}$) reached 0.99 mol/mol, indicating the complete biotransformation of EG to GA under these conditions, with a final productivity of 0.24 g/(L·h).

In the second strategy, 50 g/L of EG was introduced at the beginning of fermentation, while acetate was supplied at an initial concentration of 10 g/L (Fig. 6B). We adopted a pulse-feeding strategy for acetate, adding 10 g/L every 24 h, with a total of 30 g/L pulsed into the bioreactor. The resulting biomass was lower than that obtained in the first bioreactor experiment, reaching a final DCW of 6.2 ± 1.0 g/L (Fig. 6B). Biomass yield on acetate ($Y_{DCW/Ac}$) was higher than in the first strategy, achieving 0.21 g/g. EG was completely consumed within 60 h. The total amount of GA produced was 48.4 ± 1.4 g/L (Fig. 6B), with a final molar yield ($Y_{GA/EG}$) of 0.79 mol/mol and a productivity of 0.73 g/(L·h).

Among the bioreactor strategies tested, the pulse-feeding of acetate combined with a single high-dose EG addition at the beginning of the fermentation proved to be the most effective, yielding the highest GA production reported for yeast in a one-step fermentation process (Fig. 6B).

4. Discussion

The upcycling of molecules derived from PET depolymerization, such as EG and TPA, is emerging as a pivotal strategy in the transition towards a circular plastic economy. Unlike traditional recycling methods, which often result in downcycled products of lower quality, upcycling enables the transformation of PET-derived monomers into

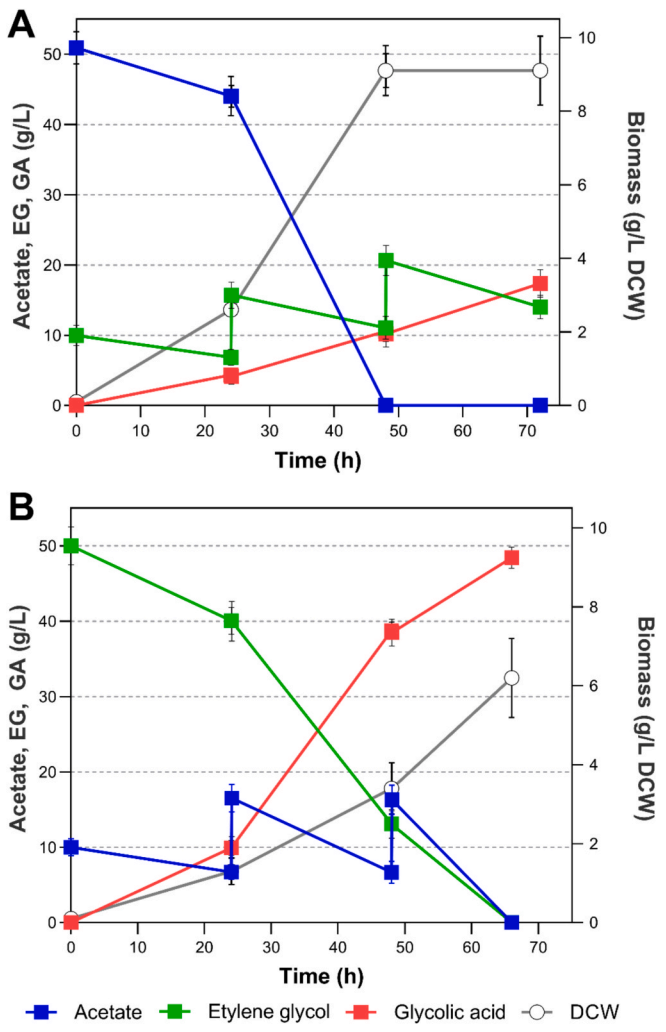

Fig. 6. Fermentation profile and GA production from EG, in 5 L bioreactors by *Y. lipolytica* Y-4972. (A) Constant Ac (50 g/L) and pulse-feeding of EG every 24 h. (B) Constant EG (50 g/L) and pulse-feeding of Ac every 24 h. The left y axis shows Ac (blue squares), EG (green squares), and GA (red squares), concentration in g/L; the right y axis shows g/L of DCW (white circles). Average and standard deviations were obtained from two independent experiments.

high-value chemicals and bioproducts, thereby enhancing both economic and environmental sustainability (Wei et al. (2020); Tiso et al., 2022). This approach not only contributes to reducing plastic waste accumulation, but also decreases dependence on fossil-derived raw materials.

In previous studies, EG has been used as a carbon source for producing biomass-related products, such as polyhydroxyalkanoates in *P. putida* (Franden et al., 2018). Alternatively, EG can be converted into value-added compounds like GA (Carniel et al., 2023; Senatore et al., 2024; Senatore et al., 2025). The present study demonstrates the successful bioconversion of EG into GA by the non-conventional yeast *Y. lipolytica*. The potential of *Y. lipolytica* as a microbial platform for EG valorization was previously explored (da Costa et al., 2020; Carniel et al., 2023). These studies demonstrated that *Y. lipolytica* can metabolize EG in nutrient-rich media such as YP. However, such media exhibit batch-to-batch variability, undefined composition, and can lead to inconsistent microbial growth and product yields. Moreover, they are susceptible to contamination, promote non-selective growth, and can lead to precipitation or growth inhibition at high concentrations (Barrette et al., 1999; Thomas and Upreti 2014; Tachibana et al., 2019; Liu et al. (2024)). Furthermore, *Y. lipolytica* can use the nutrient-rich media YP as a carbon source, so in these studies it is unclear whether the yeast can produce biomass from EG.

Our findings demonstrate that EG alone is insufficient to support *Y. lipolytica* growth in minimal medium, as the yeast is unable to utilize EG as its sole carbon source. However, EG does not exhibit toxicity toward *Y. lipolytica*, as evidenced by its ability to grow in the presence of high EG concentrations without adverse effects (Supplementary Materials). Based on previous observations in *P. putida* (Franden et al., 2018), we hypothesized that *Y. lipolytica* may oxidize EG to GA, and subsequently to glyoxylate, potentially via a putative glyoxylate oxidase (Fig. 1). Nevertheless, it is likely that glyoxylate derived from EG cannot support anabolic metabolism – particularly the synthesis of C4 intermediates – due to the absence of acetyl-CoA, which is essential for condensation with glyoxylate to form malate via malate synthase, thereby feeding the glyoxylate cycle.

To overcome this limitation, we investigated co-feeding EG with acetate, which serves as a source of acetyl-CoA. Co-utilization significantly enhanced EG consumption compared to EG alone (Table 1); however, EG uptake significantly decreased upon acetate depletion (Fig. 2A). Under Ac + EG co-culture conditions, EG was incorporated into biomass, as confirmed by ^{13}C-labeling of proteinogenic amino acids (Fig. 3B). ^{13}C-MFA analysis revealed that EG enters central metabolism via conversion to glyoxylate, which is either transaminated to glycine or incorporated into the glyoxylate cycle. During the initial co-utilization phase, approximately 7 % of EG-derived carbon was assimilated into metabolism. Labeling data further support this, showing that by the end of fermentation (168 h), nearly 50 % of glycine and serine were derived from EG (Fig. 3B). Our labeling experiments provide direct evidence for the functional importance of the alanine:glyoxylate aminotransferase encoded by gene *YlAGX1* in *Y. lipolytica*, in EG assimilation into biomass. Disruption of this gene led to a reduction of approximately 50 % in the contribution of EG to glycine and serine biosynthesis with minor effects also on other amino acids with longer carbon chains (Fig. 3C). Additionally, labeling of longer-chain amino acids demonstrates the assimilation of EG through the glyoxylate cycle (Figs. 3B, 4). Importantly, across all tested conditions, *Y. lipolytica* primarily oxidized EG to GA, with yields ranging from 0.71 to 0.99 mol/mol.

Acetate, a volatile fatty acid (VFA), is a renewable and widely available carbon source derived from various industrial processes and waste streams. Although *Y. lipolytica* exhibits a superior ability to utilize acetate compared to other yeasts, its efficient assimilation remains challenging. As reported by Liu et al. (2016), growth on acetate is limited by low uptake rates and the requirement for specific metabolic adaptations, including the activation of gluconeogenesis to generate NADPH. In *Y. lipolytica*, NADPH is primarily produced via the oxidative branch of the pentose phosphate pathway (PPP), which is fueled by glucose decarboxylation. Furthermore, elevated acetate concentrations can lead to medium alkalinization, negatively affecting biomass formation.

The introduction of EG as a co-substrate improved acetate consumption rate (Table 1), possibly by counteracting medium alkalinization through GA production, which helps the stabilization of pH. Additionally, EG oxidation likely contributes to intracellular NADPH pool, facilitating more efficient biomass accumulation and GA production. The ^{13}C-MFA data support this hypothesis by showing that EG oxidation produces NADPH (Fig. 4) at levels almost sufficient to sustain biomass formation. Consequently, reliance on the oxidative branch of the pentose phosphate pathway, which requires the energetically costly synthesis of glucose from acetate, may be reduced in the presence of EG.

These findings highlight the value of co-feeding strategies in enhancing acetate utilization by *Y. lipolytica*. Park et al. (2019) demonstrated that co-feeding gluconate with acetate improved both metabolic activity and lipid production. By introducing gluconate as a supplementary substrate, they addressed the NADPH limitation in acetate-grown cells – a key bottleneck in biosynthetic processes – by stimulating NADPH generation via the PPP. Similarly, Huang et al., (2023) employed a co-feeding approach combining glucose and acetate

with microbial electrosynthesis to supply additional reducing equivalents. This strategy significantly improved acetate assimilation and its conversion into value-added products such as fatty alcohols and triterpenoids.

The main goal of this work was to optimize GA production in a bioreactor by co-feeding EG and acetate. The most effective strategy involved introducing EG at the start while pulsing acetate every 24 h (Fig. 6B). This approach led to a GA concentration of 48.4 ± 1.4 g/L after 66 h of growth in minimal medium, achieving a molar yield of 73 % and a productivity rate of 0.73 g/(L·h). It is worth noting that these production levels could be further enhanced through targeted bioprocess engineering, as the cells remained viable and metabolically active at the end of the fermentation.

Kataoka et al., (2001) successfully produced 110 g/L of GA from EG oxidation using *Rhodotorula* sp. through a 120-hours biotransformation process. This method required, however, a high initial biomass (10.7 g of wet cell weight for a 100 ml reaction), necessitating two additional days of growth in a rich medium for accumulation. Senatore et al., (2024) produced 23.8 g/L of GA with *Scheffersomyces stipitis* in a rich medium containing glucose. Finally, the GA production previously achieved by Carniel et al., (2023) with *Y. lipolytica* was also surpassed. Cultivating *Y. lipolytica* in a rich medium for 72 h resulted in the production of 32.6 g/L of GA, with a productivity of 0.45 g/(L·h) (Carniel et al., 2023). The use of a minimal medium in our work underscores the economic advantage of our strategy, as it reduces costs while maintaining high conversion yields.

5. Conclusions

This study demonstrates the potential of *Y. lipolytica* as a microbial platform for the bioconversion of EG, a monomer derived from PET, into GA, a value-added compound. Although EG alone does not support growth in minimal medium, it is non-toxic and can be efficiently oxidized to GA when co-fed with acetate, a renewable and cost-effective carbon source. This work provides the first evidence of EG-derived carbon incorporation into biomass through a co-feeding strategy. Acetate supplies acetyl-CoA, enabling anabolic metabolism via activation of the glyoxylate cycle. ^{13}C metabolic flux analysis confirmed EG assimilation into this cycle, as well as its involvement in the biosynthesis of glycine and serine. This strategy enhanced EG uptake, GA production, and acetate utilization, likely by stabilizing pH and providing reducing equivalents for cell biosynthesis. Under optimized fed-batch conditions, 48.4 g/L of GA was produced with a 73 % molar yield and a productivity of 0.73 g/L/h. Transcriptomic analysis highlighted the significant influence of EG on transcriptional reprogramming and identified candidate enzymes that may participate in EG metabolism, providing a basis for future metabolic engineering approaches. Overall, this study provides the first demonstration of biomass formation from a plastic-derived monomer in yeast, supporting the development of scalable and sustainable PET upcycling processes within a circular bioeconomy framework.

6. Availability of data and materials

Data supporting this study are openly available from Zenodo at https://doi.org/10.5281/zenodo.17396157 . . The raw RNA-seq data have been submitted to the Sequence Read Archive (SRA – https://www.ncbi.nlm.nih.gov/sra) and are accessible under BioProject ID PRJNA1338114.

7. Declaration of generative AI and AI-assisted technologies in the manuscript preparation process

During the preparation of this work the author(s) used Microsoft Copilot to improve the grammar and phrasing. After using this tool/service, the author(s) reviewed and edited the content as needed and take(s) full responsibility for the content of the published article.

CRediT authorship contribution statement

Eugenia Messina: Writing – original draft, Validation, Methodology, Investigation, Conceptualization. **Zbigniew Lazar:** Writing – review & editing, Methodology, Conceptualization. **Serena Barile:** Writing – review & editing, Validation, Methodology, Investigation. **Paweł Moroz:** Methodology, Investigation. **Pasquale Scarcia:** Writing – review & editing. **Ylenia Antonacci:** Data curation, Methodology. **Bruno Fosso:** Data curation, Methodology. **Luigi Palmieri:** Writing – review & editing. **Isabella Pisano:** Writing – review & editing. **Gennaro Agrimi:** Writing – original draft, Validation, Supervision, Project administration, Methodology, Investigation, Conceptualization.

Declaration of competing interest

The authors declare that they have no known competing financial interests or personal relationships that could have appeared to influence the work reported in this paper.

Acknowledgments

This research was funded by the Italian Ministry of Education and Merit (MIUR) under the PRIN project No. 2020SBNHLH. Additional financial support was provided by the project “Caratterizzazione metabolica e flussomica (13C-MFA) di ceppi di lievito non convenzionali (NCY) capaci di utilizzare composti C2-C4 quali fonti di carbonio” (NCY-13CFlux), CUP H93C23001070006, funded through the public call for biodiversity monitoring, preservation, enhancement, and restoration in protected areas, as part of the “National Biodiversity Future Center (NBFC)” research program, supported by the National Recovery and Resilience Plan (PNRR), Mission 4 – Component 2 – Investment Line 1.4, and co-funded by the European Union – NEXTGENERATIONEU (Project NBFC, CUP B83C22002930006, ID CN00000033). This work also received partial support from the Italian Ministry of the Environment and Energy Security, Directorate General for Circular Economy, through the project “GreenChemBioDEP – Biocatalysis and Green Chemistry for the development of low environmental impact methodologies for the transformation of polymeric waste into renewable and reusable materials and biogas”, CUP H93C2200038000. Furthermore, funding was provided by the European Union’s Horizon Europe program under the call HORIZON-WIDERA-2023-ACCESS-02, Grant Agreement No. 101159570 (Twinn4MicroUp). Metabolomics analyses were conducted using facilities provided by ELIXIR, the European research infrastructure for life science data.

Appendix A. Supplementary material

Supplementary data to this article can be found online at https://doi.org/10.1016/j.biortech.2025.133540.

Data availability

Data supporting this study are openly available from Zenodo at https://doi.org/10.5281/zenodo.17396157. The raw RNA-seq data have been submitted to the Sequence Read Archive (SRA – https://www.ncbi.nlm.nih.gov/sra) and are accessible under BioProject ID PRJNA1338114.

References

Agrimi, G., Mena, M.C., Izumi, K., Pisano, I., Germinario, L., Fukuzaki, H., Palmieri, L., Blank, L.M., Kitagaki, H., 2014. Improved sake metabolic profile during fermentation due to increased mitochondrial pyruvate dissimilation. FEMS Yeast Res. 14 (2), 249–260. https://doi.org/10.1111/1567-1364.12120.

Ashburner, M., Ball, C.A., Blake, J.A., Botstein, D., Butler, H., Cherry, J.M., Davis, A.P., Dolinski, K., Dwight, S.S., Eppig, J.T., Harris, M.A., Hill, D.P., Issel-Tarver, L., Kasarskis, A., Lewis, S., Matese, J.C., Richardson, J.E., Ringwald, M., Rubin, G.M., Sherlock, G., 2000. Gene ontology: tool for the unification of biology. The Gene Ontology Consortium. Nat. Genet. 25 (1), 25–29. https://doi.org/10.1038/75556.

Barrette, J., Champagne, C.P., Goulet, J., 1999. Development of bacterial contamination during production of yeast extracts. Appl. Environ. Microbiol. 65 (7), 3261–3263. https://doi.org/10.1128/AEM.65.7.3261-3263.1999.

Carniel, A., Santos, A.G., Chinelatto, L.S., Castro, A.M., Coelho, M.A.Z., 2023. Biotransformation of ethylene glycol to glycolic acid by *Yarrowia lipolytica*: a route for poly(ethylene terephthalate) (PET) upcycling. Biotechnol. J. 18 (6), e2200521. https://doi.org/10.1002/biot.202200521.

Ceven, E.K., Karakan Gunaydin, G., 2023. Global trends for fibre production and marketing. Int. Conf. Trends Adv. Res. 1, 255–262 (Accessed: 2 September 2025).

Charest, J., Loebenstein, P., Mach, R.L., Mach-Aigner, A.R., 2025. FunFEA: an R package for fungal functional enrichment analysis. BMC Bioinf. 26 (1), 138. https://doi.org/10.1186/s12859-025-06164-7.

Chauhan, S., DiCosimo, R., Fallon, R.D., Gavagan, J.E., 2002. Payne M.S. Method for producing glycolic acid from glycolonitrile using nitrilase. US6416980B1.

Chen, Q., Chen, Y., Hou, Z., Ma, Y., Huang, J., Zhang, Z., Chen, Y., Yang, X., Zhang, Y., Zhao, G., 2024. Unlocking the formate utilization of wild-type *Yarrowia lipolytica* through adaptive laboratory evolution. Biotechnol. J. 19 (6), e2400290. https://doi.org/10.1002/biot.202400290.

Christensen, B., Nielsen, J., 2002. Reciprocal ^{13}C-labeling: a method for investigating the catabolism of cosubstrates. Biotechnol. Prog. 18 (2), 163–166. https://doi.org/10.1021/bp010152d.

Ciliberti, C., Biundo, A., Albergo, R., Agrimi, G., Braccio, G., de Bari, I., Pisano, I., 2020. Syngas derived from lignocellulosic biomass gasification as an alternative resource for innovative bioprocesses. Processes 8 (12), 1567. https://doi.org/10.3390/pr8121567.

da Costa, A.M., de Oliveira Lopes, V.R., Vidal, L., Nicaud, J.M., de Castro, A.M., Coelho, M.A.Z., 2020. Poly(ethylene terephthalate) (PET) degradation by *Yarrowia lipolytica*: investigations on cell growth, enzyme production and monomers consumption. Process Biochem. 95, 81–90. https://doi.org/10.1016/j.procbio.2020.04.001.

Franden, M.A., Jayakody, L.N., Li, W.J., Wagner, N.J., Cleveland, N.S., Michener, W.E., Hauer, B., Blank, L.M., Wierckx, N., Klebensberger, J., Beckham, G.T., 2018. Engineering *Pseudomonas putida* KT2440 for efficient ethylene glycol utilization. Metab. Eng. 48, 197–207. https://doi.org/10.1016/j.ymben.2018.06.003.

García, J.L., 2022. Enzymatic recycling of polyethylene terephthalate through the lens of proprietary processes. J. Microbial. Biotechnol. 15, 2699–2704. https://doi.org/10.1111/1751-7915.14114.

Gene Ontology Consortium, Aleksander, S.A., Balhoff, J., Carbon, S., Cherry, J.M., Drabkin, H.J., Ebert, D., Feuermann, M., Gaudet, P., Harris, N.L., Hill, D.P., Lee, R., Mi, H., Moxon, S., Mungall, C.J., Muruganugan, A., Mushayahama, T., Sternberg, P. W., Thomas, P.D., Van Auken, K., Westerfield, M., 2023. The gene ontology knowledgebase in 2023. Genetics 224 (1), iyad031. https://doi.org/10.1093/genetics/iyad031.

Gomez, J.D., Wall, M.L., Rahim, M., Kambhampati, S., Evans, B.S., Allen, D.K., Antoniewicz, M.R., Young, J.D., 2023. Program for integration and rapid analysis of mass isotopomer distributions (PIRAMID). Bioinformatics 39 (11). https://doi.org/10.1093/bioinformatics/btad661.

Huang, C., Chen, Y., Cheng, S., Li, M., Wang, L., Cheng, M., Li, F., Cao, Y., Song, H., 2023. Enhanced acetate utilization for value-added chemicals production in *Yarrowia lipolytica* by integration of metabolic engineering and microbial electrosynthesis. Biotechnol. Bioeng. 120 (10), 3013–3024. https://doi.org/10.1002/bit.28465.

Ilyas, M., Ahmad, W., Khan, H., Yousaf, S., Khan, K., Nazir, S., 2018. Plastic waste as a significant threat to environment - a systematic literature review. Rev. Environ. Health 33 (4), 383–406. https://doi.org/10.1515/reveh-2017-0035.

Kanehisa, M., Goto, S., 2000. KEGG: kyoto encyclopedia of genes and genomes. Nucleic Acids Res. 28 (1), 27–30. https://doi.org/10.1093/nar/28.1.27.

Kataoka, M., Sasaki, M., Hidalgo, A.R., Nakano, M., Shimizu, S., 2001. Glycolic acid production using ethylene glycol-oxidizing microorganisms. Biosci. Biotech. Bioch. 65 (10), 2265–2270. https://doi.org/10.1271/bbb.65.2265.

Kersters, K., De Ley, J., 1963. The oxidation of glycols by acetic acid bacteria. BBA 71, 311–331. https://doi.org/10.1016/0006-3002(63)91086-2.

Kwon, G., Cho, D.W., Park, J., Bhatnagar, A., Song, H., 2023. A review of plastic pollution and their treatment technology: a circular economy platform by thermochemical pathway. Chem. Eng. J. 464. https://doi.org/10.1016/j.cej.2023.142771.

Li, W.J., Jayakody, L.N., Franden, M.A., Wehrmann, M., Daun, T., Hauer, B., Blank, L.M., Beckham, G.T., Klebensberger, J., Wierckx, N., 2019. Laboratory evolution reveals the metabolic and regulatory basis of ethylene glycol metabolism by *Pseudomonas putida* KT2440. Environ. Microbiol. 21 (10), 3669–3682. https://doi.org/10.1111/1462-2920.14703.

Liao, Y., Smyth, G.K., Shi, W., 2019. The R package Rsubread is easier, faster, cheaper and better for alignment and quantification of RNA sequencing reads. Nucleic Acids Res. 47 (8), e47.

Liu, N., Qiao, K., Stephanopoulos, G., 2016. ^{13}C metabolic flux analysis of acetate conversion to lipids by *Yarrowia lipolytica*. Metab. Eng. 38, 86–97. https://doi.org/10.1016/j.ymben.2016.06.006.

Liu, G., Tiang, M.F., Ma, S., Wei, Z., Liang, X., Sajab, M.S., Abdul, P.M., Zhou, X., Ma, Z., Ding, G., 2024. An alternative peptone preparation using Hermetia illucens (Black soldier fly) hydrolysis: process optimization and performance evaluation. PeerJ 12, e16995. https://doi.org/10.7717/peerj.16995.

Lomwongsopon, P., Varrone, C., 2022. Critical review on the progress of plastic bioupcycling technology as a potential solution for sustainable plastic waste management. Polymers 14 (22), 4996. https://doi.org/10.3390/polym14224996.

Messina, E., de Souza, C.P., Cappella, C., Barile, S.N., Scarcia, P., Pisano, I., Palmieri, L., Nicaud, J.M., Agrimi, G., 2023. Genetic inactivation of the Carnitine/Acetyl-Carnitine mitochondrial carrier of *Yarrowia lipolytica* leads to enhanced odd-chain fatty acid production. Microb. Cell Fact. 22 (1), 128. https://doi.org/10.1186/s12934-023-02137-8.

Mückschel, B., Simon, O., Klebensberger, J., Graf, N., Rosche, B., Altenbuchner, J., Pfannstiel, J., Huber, A., Hauer, B., 2012. Ethylene glycol metabolism by *Pseudomonas putida*. Appl. Environ. Microbiol. 78 (24), 8531–8539. https://doi.org/10.1128/AEM.02062-12.

Muringayil Joseph, T., Azat, S., Ahmadi, Z., Moini Jazani, O., Esmaeili, A., Kianfar, E., Haponiuk, J., Thomas, S., 2024. Polyethylene terephthalate (PET) recycling: a review. Case Stud. Chem. Environ. Eng. 9. https://doi.org/10.1016/j.cscee.2024.100673.

Mutyala, S., Kim, J.R., 2022. Recent advances and challenges in the bioconversion of acetate to value-added chemicals. Bioresour. Technol. 364, 128064. https://doi.org/10.1016/j.biortech.2022.128064.

Nayanathara Thathsarani Pilapitiya, P.G.C., Ratnayake, A.S., 2024. The world of plastic waste: a review. Cleaner Mater. 11. https://doi.org/10.1016/j.clema.2024.100220.

Pan, P., Hua, Q., 2012. Reconstruction and in silico analysis of metabolic network for an oleaginous yeast. Yarrowia Lipolytica. Plos One 7 (12), e51535. https://doi.org/10.1371/journal.pone.0051535.

Park, J.O., Liu, N., Holinski, K.M., Emerson, D.F., Qiao, K., Woolston, B.M., Xu, J., Lazar, Z., Islam, M.A., Vidoudez, C., Girguis, P.R., Stephanopoulos, G., 2019. Synergistic substrate cofeeding stimulates reductive metabolism. Nature Metabol. 1 (6), 643–651. https://doi.org/10.1038/s42255-019-0077-0.

Park, Y.K., González-Fernández, C., Robles-Iglesias, R., Vidal, L., Fontanille, P., Kennes, C., Tomás Pejó, E., Nicaud, J.M., Fickers, P., 2021. Bioproducts generation from carboxylate platforms by the non-conventional yeast *Yarrowia lipolytica*. FEMS Yeast Res. 21 (6), foab047. https://doi.org/10.1093/femsyr/foab047.

Salusjärvi, L., Havukainen, S., Koivistoinen, O., Toivari, M., 2019. Biotechnological production of glycolic acid and ethylene glycol: current state and perspectives. Appl. Microbiol. Biotechnol. 103 (6), 2525–2535. https://doi.org/10.1007/s00253-019-09640-2.

Schlösser, T., Gätgens, C., Weber, U., Stahmann, K.P., 2004. Alanine: Glyoxylate aminotransferase of *Saccharomyces cerevisiae*-encoding gene AGX1 and metabolic significance. Yeast 21 (1), 63–73. https://doi.org/10.1002/yea.1058.

Schmitz, A., Ebert, B.E., Blank, L.M., 2015. GC-MS-based determination of mass isotopomer distributions for ^{13}C-based metabolic flux analysis. In: McGenity, T., Timmis, K., Nogales, B. (Eds.), Hydrocarbon and Lipid Microbiology Protocols. Springer Protocols Handbooks. Springer, Berlin, Heidelberg, pp. 223–243. https://doi.org/10.1007/8623_2015_78.

Senatore, V.G., Masotti, F., Milanesi, R., Ceccarossi, S., Maestroni, L., Serra, I., Branduardi, P., 2025. Challenges in elucidating ethylene glycol metabolism in *Saccharomyces cerevisiae*. FEMS Yeast Res. 25, foaf006. https://doi.org/10.1093/femsyr/foaf006.

Senatore, V.G., Milanesi, R., Masotti, F., Maestroni, L., Pagliari, S., Cannavacciuolo, C., Campone, L., Serra, I., Branduardi, P., 2024. Exploring yeast biodiversity and process conditions for optimizing ethylene glycol conversion into glycolic acid. FEMS Yeast Res. 24. https://doi.org/10.1093/femsyr/foae024.

Si, D., Xiong, B., Chen, L., Shi, J., 2021. Highly selective and efficient electrocatalytic synthesis of glycolic acid in coupling with hydrogen evolution. Chem Catal. 1 (4), 941–955. https://doi.org/10.1016/j.checat.2021.08.001.

Tachibana, S., Watanabe, K., Konishi, M., 2019. Estimating effects of yeast extract compositions on *Escherichia coli* growth by a metabolomics approach. J. Biosci. Bioeng. 128 (4), 468–474. https://doi.org/10.1016/j.jbiosc.2019.03.012.

Tatusov, R.L., Fedorova, N.D., Jackson, J.D., Jacobs, A.R., Kiryutin, B., Koonin, E.V., Krylov, D.M., Mazumder, R., Mekhedov, S.L., Nikolskaya, A.N., Rao, B.S., Smirnov, S., Sverdlov, A.V., Vasudevan, S., Wolf, Y.I., Yin, J.J., Natale, D.A., 2003. The COG database: an updated version includes eukaryotes. BMC Bioinf. 4, 41. https://doi.org/10.1186/1471-2105-4-41.

Thomas, P., Upreti, R., 2014. Significant effects due to peptone in kelman medium on colony characteristics and virulence of *Ralstonia solanacearum* in tomato. Open Microbiol J. 31 (8), 95–114. https://doi.org/10.2174/1874285801408010095.

Tiso, T., Winter, B., Wei, R., Hee, J., de Witt, J., Wierckx, N., Quicker, P., Bornscheuer, U. T., Bardow, A., Nogales, J., Blank, L.M., 2022. The metabolic potential of plastics as biotechnological carbon sources – review and targets for the future. Metab. Eng. 71, 77–98. https://doi.org/10.1016/j.ymben.2021.12.006.

Weber, E., Engler, C., Gruetzner, R., Werner, S., Marillonnet, S., 2011. A modular cloning system for standardized assembly of multigene constructs. PLoS One 6 (2), e16765. https://doi.org/10.1371/journal.pone.0016765.

Wei, G., Yang, X., Gan, T., Zhou, W., Lin, J., Wei, D., 2009. High cell density fermentation of *Gluconobacter oxydans* DSM 2003 for glycolic acid production. J. Ind. Microbiol. Biotechnol. 36 (8), 1029–1034. https://doi.org/10.1007/s10295-009-0584-1.

Wei, R., Tiso, T., Bertling, J., O'Connor, K., Blank, L.M., Bornscheuer, U.T., 2020. Possibilities and limitations of biotechnological plastic degradation and recycling. Nat. Catal. 3, 867–871. https://doi.org/10.1038/s41929-020-00521-w.

Worland, A.M., Han, Z., Maruwan, J., Wang, Y., Du, Z.Y., Tang, Y.J., Su, W.W., Roell, G. W., 2024. Elucidation of triacylglycerol catabolism in *Yarrowia lipolytica*: how cells balance acetyl-CoA and excess reducing equivalents. Metab. Eng. 85, 1–13. https://doi.org/10.1016/j.ymben.2024.06.010.

Young, J.D., 2014. INCA: a computational platform for isotopically non-stationary metabolic flux analysis. Bioinformatics (oxford, England) 30 (9), 1333–1335. https://doi.org/10.1093/bioinformatics/btu015.

Yuzbashev, T.V., Yuzbasheva, E.Y., Melkina, O.E., Patel, D., Bubnov, D., Dietz, H., Ledesma-Amaro, R., 2023. A DNA assembly toolkit to unlock the CRISPR/Cas9 potential for metabolic engineering. Commun. Biol. 6 (1), 858. https://doi.org/10.1038/s42003-023-05202-5.

Zhang, H., Shi, L., Mao, X., Lin, J., Wei, D., 2016. Enhancement of cell growth and glycolic acid production by overexpression of membrane-bound alcohol dehydrogenase in *Gluconobacter oxydans* DSM 2003. J. Biotechnol. 237, 18–24. https://doi.org/10.1016/j.jbiotec.2016.09.003.

Zhao, X., Boruah, B., Chin, K.F., Đokić, M., Modak, J.M., Soo, H.S., 2022. Upcycling to sustainably reuse plastics. Adv. Mater. (deerfield Beach, Fla.) 34 (25), e2100843. https://doi.org/10.1002/adma.202100843.

Zhu, J., Shao, W., Li, X., Jiao, X., Zhu, J., Sun, Y., Xie, Y., 2021. Asymmetric triple-atom sites confined in ternary oxide enabling selective CO_2 photothermal reduction to acetate. J. Am. Chem. Soc. 143 (43), 18233–18241. https://doi.org/10.1021/jacs.1c08033.